*Evolution*, 54(4), 2000, pp. 1102–1115

# COEVOLUTIONARY CLINES ACROSS SELECTION MOSAICS

SCOTT L. NUISMER,[1,2] JOHN N. THOMPSON,[1,3] AND RICHARD GOMULKIEWICZ[1,4]
[1]*School of Biological Sciences, P.O. Box 644234, Washington State University, Pullman, Washington 99164*
[2]*E-mail: nuismer@wsu.edu*
[4]*Department of Pure and Applied Mathematics, P.O. Box 643113, Washington State University, Pullman, Washington 99164*

*Abstract.*—Much of the dynamics of coevolution may be driven by the interplay between geographic variation in reciprocal selection (selection mosaics) and the homogenizing action of gene flow. We develop a genetic model of geographically structured coevolution in which gene flow links coevolving communities that may differ in both the direction and magnitude of reciprocal selection. The results show that geographically structured coevolution may lead to allele-frequency clines within both interacting species when fitnesses are spatially uniform or spatially heterogeneous. Furthermore, the results show that the behavior and shape of clines differ dramatically among different types of coevolutionary interaction. Antagonistic interactions produce dynamic clines that change shape rapidly through time, producing shifting patterns of local adaptation and maladaptation. Unlike antagonistic interactions, mutualisms generate stable equilibrium patterns that lead to fixed spatial patterns of adaptation. Interactions that vary between mutualism and antagonism produce both equilibrium and dynamic clines. Furthermore, the results demonstrate that these interactions may allow mutualisms to persist throughout the geographic range of an interaction, despite pockets of locally antagonistic selection. In all cases, the coevolved spatial patterns of allele frequencies are sensitive to the relative contributions of gene flow, selection, and overall habitat size, indicating that the appropriate scale for studies of geographically structured coevolution depends on the relative contributions of each of these factors.

*Key words.*—Antagonism, clines, coevolution, gene flow, geographic mosaic theory, local adaptation, maladaptation, mutualism.

Received October 13, 1999. Accepted March 7, 2000.

Many natural populations show geographic clines in traits including morphology, gene frequencies, behavior, and patterns of adaptation and maladaptation. The evolutionary forces that give rise to these single-species clines have been the subject of much theoretical and experimental work, with most studies focusing on clines maintained either by adaptation to different environments (Haldane 1948; Fisher 1950; Endler 1973; Slatkin 1973; Nagylaki 1975; Garcia-Ramos and Kirkpatrick 1997), or by selection against hybrids (Bazykin 1969; Barton and Hewitt 1985; Campbell et al. 1997; Gavrilets 1997). This work has led to a well-developed theory for single-species clines, including the effects of multiple loci (Li and Nei 1974; Slatkin 1975; Barton 1983, 1999; Kruuk et al. 1999) variable population densities (Barton 1979; Kirkpatrick and Barton 1997), and intraspecific frequency-dependent selection (Mallet and Barton 1989). Although many single-species clines are surely produced by these processes, relatively little is known about the structure and dynamics of clines within those species whose evolution is governed primarily by interspecific interactions. For many host-parasite and host-symbiont interactions, the potential clearly exists for coevolution between the interacting species to be the primary factor governing geographic variation across landscapes.

The role of coevolution in shaping spatial patterns of variation in interacting species has developed rapidly as studies designed to test predictions of the geographic mosaic theory of coevolution (Thompson 1994, 1999a) and related views of coevolution have begun to accumulate. The theory argues that much of ongoing coevolution may result from the interplay of selection mosaics (where the fitnesses of interacting species vary geographically) and shifting genetic landscapes shaped by gene flow, genetic drift, and the dynamics of extinction and recolonization (Thompson 1999b). Empirical support now exists for the primary components of a geographic mosaic view, including selection mosaics and spatial patterns of local maladaptation caused by gene flow among populations of interacting species. Evidence for selection mosaics has accumulated for a wide range of taxa and types of interaction, including those between seed-eating crossbills and pines, a sterilizing trematode and its snail host, *Drosophila* and its parasitoids, and *Taricha* salamanders and garter snakes (Benkman 1999; Brodie and Brodie 1999; Kraaijeveld and Godfray 1999; Lively 1999). As the empirical evidence for selection mosaics has increased, so to has support for the role of gene flow in shaping spatial patterns of maladaptation within species interactions (Berenbaum and Zangerl 1998; Storfer and Sih 1998; Kaltz et al. 1999; Lively 1999; Parker 1999). This emerging pattern of empirical evidence argues strongly for a geographic view of coevolution and for the potentially dynamic role of coevolution in shaping the spatial pattern of traits important to species interactions.

As the empirical evidence for the importance of coevolution in shaping spatial patterns of variation has increased, so too have the number of theoretical investigations into the causes and consequences of geographically structured coevolution. Gandon et al. (1996) modeled explicit space and extinction-recolonization dynamics in an analysis of local adaptation in a host-parasite metapopulation. Their results demonstrated that patterns of local adaptation and maladaptation can be strongly affected by spatial structure even in a completely homogenous environment. This model also demonstrated that asymmetric gene flow between hosts and parasites can have strong effects on patterns of adaptation, with relatively higher levels of parasite gene flow promoting local adaptation of parasites. When environmental hetero-

[3] Present address: Ecology and Evolutionary Biology Group, Department of Biology, University of California, Santa Cruz, California 95064.

geneity was recently incorporated into a different model of predator-prey coevolution, organized patterns of maladaptation and selection mosaics emerged (Hochberg and van Baalen 1998). A gradient in prey productivity in the model produced results indicating that reciprocal selection would be most intense in regions of highest prey productivity, thus potentially creating a selection mosaic. More recently, work that has explicitly incorporated selection mosaics into a spatially structured genetic model showed that novel coevolutionary dynamics, equilibria, and patterns of local maladaptation readily emerge (Nuismer et al. 1999). Collectively, these models have begun to elucidate how geographic structure can alter coevolutionary dynamics by building on previous genetic models of coevolution within panmictic interactions (Seger 1988; Frank 1993; Gavrilets and Hastings 1998) and interactions with implicit spatial structure (Frank 1997; Leonard 1997).

Here we extend this theoretical framework by formulating a spatially explicit genetic model of two coevolving species that are distributed as semi-isolated interacting populations arranged along a single spatial axis. Our model allows for spatially homogenous fitnesses as well as three distinct types of selection mosaics. We first consider purely antagonistic interactions, such as those between hosts and parasites or between predators and prey. We use the model to investigate both spatially homogenous environments, where reciprocal selection is constant, and spatially heterogeneous environments, where reciprocal selection varies from strong antagonism within some regions to weak antagonism in others. Antagonistic selection mosaics have been shown to arise readily when there is spatial variation in patterns of parasitoid virulence (Kraaijeveld and Godfray 1999), spatial variation in risk of infection (Lively 1999), and spatial variation in underlying ecological properties (Hochberg and van Baalen 1998). We then consider purely mutualistic interactions, such as those between some rhizobia and their host plants (e.g., Parker 1999). We use the model to investigate both spatially homogeneous environments and heterogeneous environments where geographic regions vary in the extent to which an interaction is beneficial to both species involved. Finally, we consider interactions that vary geographically between mutualistic and antagonistic selection. Interactions that have the potential to shift between mutualism and antagonism have been demonstrated for a variety of systems and may be important for understanding the conditions that lead to the evolution of obligate mutualisms (Munger and Holmes 1987; Maschinski and Whitham 1989; Nguyen et al. 1989; Michalakis et al. 1992; Thompson and Pellmyr 1992; Thompson 1994; Saikkonen et al. 1998).

For each of these three types of interaction, we use our model to address four important questions on how geographically structured coevolution may shape geographic patterns of variation: (1) Can polymorphic clines coevolve in the absence of selection mosaics? (2) Do selection mosaics promote the formation and persistence of polymorphic clines? (3) What combinations of selection, gene flow, and habitat size are most likely to lead to clines? (4) Does geographically structured coevolution lead to predictable patterns of local maladaptation?

## Model Description

### *Discrete Time and Space*

Here we describe a discrete time and space model for two coevolving species that are distributed identically across a landscape as a series of interacting populations connected by gene flow. The model allows reciprocal selection to vary in both sign and magnitude across these interacting populations, permitting virtually any spatial pattern of reciprocal selection. We simplify the genetics of coevolution by assuming that both species are haploid, with two alternative alleles at a single locus governing the dynamics of coevolution. Species 1, the parasite or mutualistic symbiont, has alleles Y and y, with frequencies at each geographic position $i$ given by $p_{1,i}$ and $(1 - p_{1,i})$, respectively, whereas species 2, the host, has alleles Z and z, with frequencies $p_{2,i}$ and $(1 - p_{2,i})$, respectively. For simplicity and to facilitate comparison with previous work, we use a simple matching alleles model to describe coevolution at a specific geographic location (Seger 1988; Gavrilets and Hastings 1998). With such a model, interactions that affect fitness occur only when individuals carrying matching alleles, such as Y and Z, meet. When pairwise interactions between two species occur at random, this matching alleles model leads naturally to fitness functions that are both linear and symmetric. For a single geographic location $i$, the fitnesses are:

$$W_{Y,i} = 1 + c_i p_{2,i}, \tag{1a}$$

$$W_{y,i} = 1 + c_i(1 - p_{2,i}), \tag{1b}$$

$$W_{Z,i} = 1 + b_i p_{1,i}, \quad \text{and} \tag{1c}$$

$$W_{z,i} = 1 + b_i(1 - p_{1,i}), \tag{1d}$$

where $W_{k,i}$ is the fitness of genotype $k$ at location $i$, $c_i$ is the fitness sensitivity of species 1 (the mutualistic symbiont or parasite) at location $i$ to changes in the frequency of its matching allele in species 2 (the host) at location $i$, and $b_i$ is the fitness sensitivity of species 2 at location $i$ to changes in the frequency of its matching allele in species 1 at location $i$. Assuming both mutation and genetic drift are weak relative to selection, the allele frequencies at a single location after one round of coevolutionary selection, but before migration, are:

$$p^*_{1,i} = \frac{p_{1,i}W_{Y,i}}{p_{1,i}W_{Y,i} + (1 - p_{1,i})W_{y,i}} \quad \text{and} \tag{2a}$$

$$p^*_{2,i} = \frac{p_{2,i}W_{Z,i}}{p_{2,i}W_{Z,i} + (1 - p_{2,i})W_{z,i}}, \tag{2b}$$

where $p^*_{k,i}$ is the postselection allele frequency for species $k$ at position $i$. When either $c_i > 0$, $b_i < 0$ or $c_i < 0$, $b_i > 0$ the interaction is antagonistic, and one species benefits from interacting while the other is harmed. Positive values of both $b_i$ and $c_i$ indicate a mutualistic interaction. If an interaction were antagonistic at an isolated location $i$, allele frequencies would oscillate in both interacting species, with the amplitude of these oscillations increasing through time and eventually leading to fixation in finite populations (Seger 1988). The stronger the reciprocal fitness effects of the interaction (i.e., larger magnitudes of parameters $c_i$ and $b_i$), the more rapidly

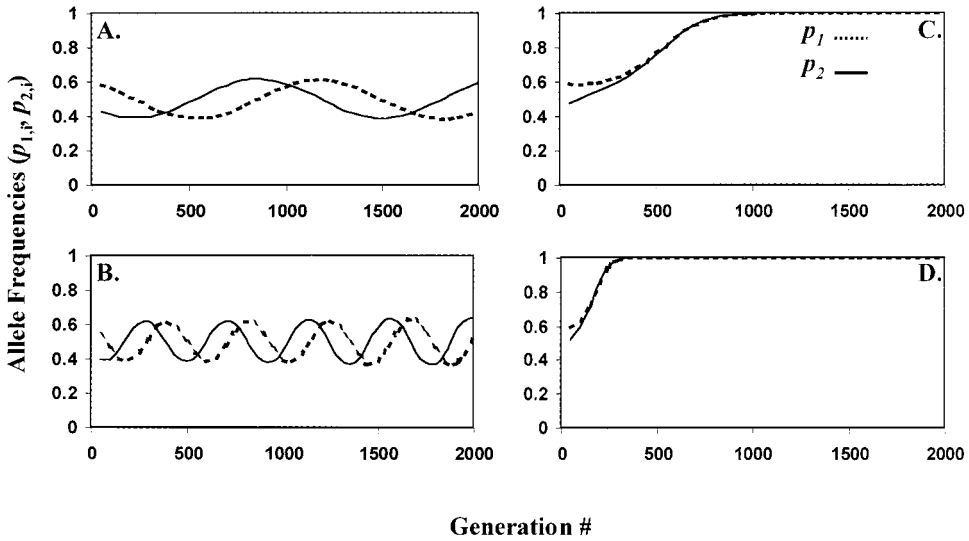


FIG. 1. Dynamics of coevolution at a single discrete geographic location, *i*, determined from numerical simulation of equations (2a,b) with initial frequencies $p_{1,i} = 0.6$ and $p_{2,i} = 0.45$ (A) Weak antagonistic selection ($c_i = 0.01$, $b_i = -0.01$) resulting in oscillations that show no noticeable increases in amplitude through time. (B) Stronger antagonistic selection ($c_i = 0.03$, $b_i = -0.03$) leading to oscillations that increase in amplitude through time. (C) Relatively weak mutualistic selection ($c_i = 0.01$, $b_i = 0.01$) leading to fixation of matching alleles over roughly 1100 generations. (D) Stronger mutualistic selection ($c_i = 0.03$, $b_i = 0.03$) leading to the more rapid fixation of matching alleles over roughly 400 generations.

the amplitude of oscillations increases (Fig. 1A,B). If an interaction were mutualistic at a location *i*, positive frequency dependence would lead to the fixation of matching alleles. The rate of fixation is primarily determined by the strength of reciprocal selection, with stronger selection (i.e., larger magnitudes of parameters $c_i$ and $b_i$) leading to more rapid fixation (Fig. 1C,D).

We incorporated geographic structure into this single-patch model by imagining discrete populations of interacting species uniformly distributed at *n* locations along a single spatial dimension. We assume gene flow is constant through time, symmetric in space, independent of local fitness (i.e., soft selection), and occurs after selection. Furthermore, we assume that in every generation each population of species *k* at position *i* is composed of a proportion of migrants $M_k(i, j)$ from population *j*. With these assumptions the allele frequencies at each discrete geographic location, *i*, after one round of selection and gene flow are:

$$p'_{k,i} = \sum_{j=1}^{n} M_k(i, j) p^*_{k,j}, \tag{3}$$

where *n* is the total number of populations and $p^*_{k,j}$ is the postselection allele frequency of species *k* at each location *j*, calculated from equations (2). Although equation (3) assumes no particular migration scheme, we will restrict our consideration to Gaussian migration of the form:

$$M_k(i, j) = \frac{\exp\left[-\frac{1}{2}\left(\frac{j - i}{\sigma_k}\right)^2\right]}{\sum_{j=1}^{n} \exp\left[-\frac{1}{2}\left(\frac{j - i}{\sigma_k}\right)^2\right]}, \tag{4}$$

where $\sigma_k^2$ is the migration variance of species *k*, for $k = 1$, 2. Definition (4) indicates that the proportion of population *i* composed of migrants from population *j* decreases with the distance between *i* and *j*, and increases with larger values of the migration variance $\sigma_k^2$.

We use the discrete time and space recursion equations (1)–(4) to simulate coevolution in spatially homogenous environments, by assuming $b_i$ and $c_i$ are constant throughout the geographic range of the interaction. Selection mosaics are modeled by allowing $b_i$ and $c_i$ to vary with location. Our treatment of selection mosaics will be limited to ''step clines,'' where the *n* linearly distributed populations are divided into two arbitrary regions, with $c_i$ and $b_i$ taking the constant values $c_L$ and $b_L$ in the left-hand region $\{-A < i < 0\}$ and $c_R$ and $b_R$ in the right-hand region $\{0 < i < B\}$ (Fig. 2). This model structure allows a wide variety of coevolutionary interactions within spatial regions (e.g., mutualism, antagonism, or commensalism) and any combination of types across regions (Fig. 2).

### *Diffusion Approximation*

To provide a more extensive analysis than is possible with the purely discrete model, we use a diffusion approximation to this model. When selection is weak, Gavrilets and Hastings (1998) have shown that the dynamics of coevolution at an isolated geographic location, described by equations (2), can be approximated in continuous time with the system of differential equations,

$$\frac{p_1(x, t)}{t} \approx c(x) p_1 (1 - p_1)(2p_2 - 1) \quad \text{and} \tag{5a}$$

$$\frac{p_2(x, t)}{t} \approx b(x) p_2 (1 - p_2)(2p_1 - 1), \tag{5b}$$

where the discrete spatial positions, *i*, have been replaced by their continuous analog, *x*, and the arguments of $p_1(x, t)$ and $p_2(x, t)$ have been suppressed on the right-hand side for no-

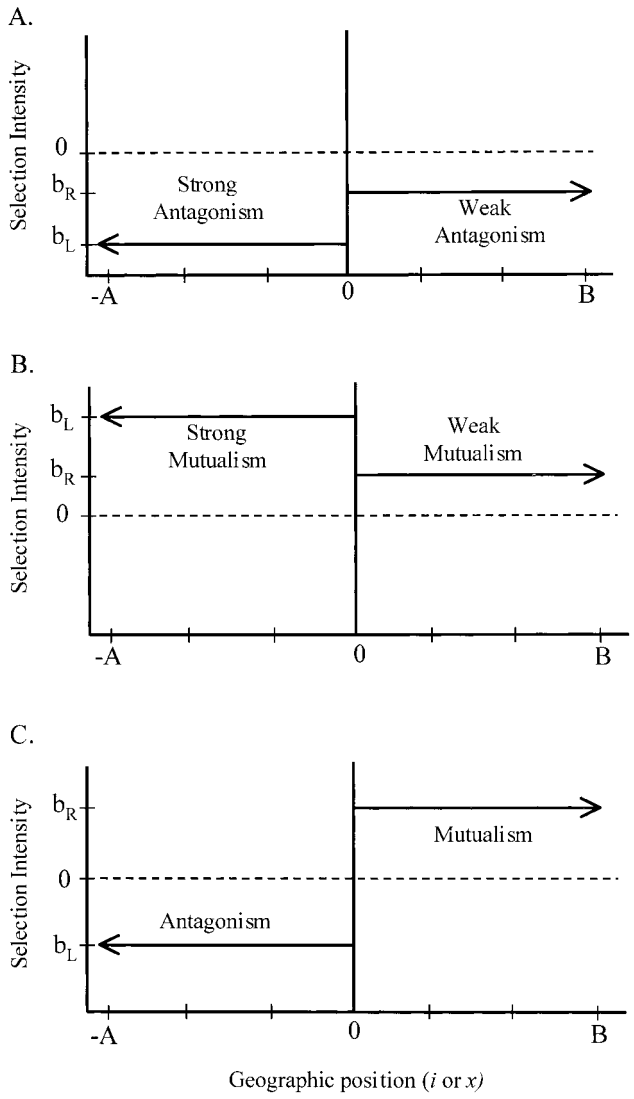


FIG. 2. A schematic diagram of the spatial structure of selection on the host species for three types of selection mosaics. The dashed line indicates the point at which there is no selection. (A) An antagonistic interaction with different selection sensitivities ($b_L$ and $b_R$) experienced by the host species within the two spatial regions. (B) A mutualistic interaction with different levels of selection on the host ($b_L$ and $b_R$) between the two spatial regions. (C). An interaction that varies between antagonism and mutualism between the two spatial regions. Selection on the host is positive within the mutualistic region and negative within the antagonistic region.

tational clarity. The coevolutionary dynamics produced by this continuous time approximation differ from those of the original discrete model by producing stable cycles in antagonistic interactions, rather than expanding oscillations. However, numerical simulation of the discrete time and space recursion equations (2) indicates that for small magnitudes of $b_i$ and $c_i$ the qualitative dynamics of the discrete and continuous models are indistinguishable, even over relatively long time scales (e.g., 5000 generations).

We incorporate space into our approximation by adapting the diffusion approximation originally suggested by Fisher (1937) for the geographic spread of an advantageous allele within a single species. This approximation has been used frequently in investigations of clines within single species (e.g., Bazykin 1969; Mallet and Barton 1989; Gavrilets 1997) and has been extensively tested numerically by Slatkin (1973), who found that the diffusion approximation and the original discrete model were in good agreement for weak selection. Nagylaki (1975) has also provided a rigorous derivation of the diffusion approximation, and shown that the approximation is valid when: (1) populations are distributed continuously across space: (2) selection is weak; and (3) gene flow is constant through time and symmetrical in space. This rigorous theoretical basis established for the single-species case suggests an appropriate approximation to the discrete time and space coevolutionary model described by equations (1)–(4). Using equations (5) and the assumptions of Nagylaki (1975), we approximate geographically structured coevolution with the partial differential equations:

$$\frac{\partial p_1(x,\,t)}{\partial t} = \frac{l_1^2}{2}\frac{\partial^2}{\partial x^2}p_1 + c(x)p_1(1 - p_1)(2p_2 - 1) \qquad \{-\mathrm{A} < x < \mathrm{B}\} \tag{6a}$$

and

$$\frac{\partial p_2(x,\,t)}{\partial t} = \frac{l_2^2}{2}\frac{\partial^2}{\partial x^2}p_2 + b(x)p_2(1 - p_2)(2p_1 - 1), \qquad \{-\mathrm{A} < x < \mathrm{B}\} \tag{6b}$$

where $l_1^2$ and $l_2^2$ are migration variances analogous to $\sigma_1^2$ and $\sigma_2^2$ in the discrete model and the variable $x$ is position along a continuous, one-dimensional spatial axis that extends from $-$A to B. In all cases, we will assume the zero flux boundary conditions for equations (6). When fitnesses are spatially homogenous, both $b(x)$ and $c(x)$ are constant throughout the geographic range of the interaction. As in the discrete model, selection mosaics will assume a step cline with $c(x)$ and $b(x)$ given by the constants $c_L$ and $b_L$ in the left-hand region $\{-\mathrm{A} < x < 0\}$ and $c_R$ and $b_R$ in the right-hand region $\{0 < x < \mathrm{B}\}$.

Equilibrium patterns of the allele frequencies $p_1(x,t)$ and $p_2(x,t)$ can be determined by setting equations (6) equal to zero and solving the resulting ordinary differential equations. If we let $\hat{p}_1(x)$ and $\hat{p}_2(x)$ denote equilibrium allele frequencies and define $\omega_1(x) = 2c(x)/l_1^2$ and $\omega_2(x) = 2b(x)/l_2^2$, then we have:

$$\frac{d^2\hat{p}_1(x)}{dx^2} = -\omega_1(x)\hat{p}_1(1 - \hat{p}_1)(2\hat{p}_2 - 1) \qquad \{-\mathrm{A} < x < \mathrm{B}\} \tag{7a}$$

and

$$\frac{d^2\hat{p}_2(x)}{dx^2} = -\omega_2(x)\hat{p}_2(1 - \hat{p}_2)(2\hat{p}_1 - 1), \qquad \{-\mathrm{A} < x < \mathrm{B}\} \tag{7b}$$

where we will again assume the zero flux boundary conditions. For any given type of coevolutionary selection, there are always equilibria, $\hat{p}_1(x)$ and $\hat{p}_2(x)$, with spatially uniform allele frequencies in both interacting species (Table 1). We use the equilibrium equations (7) and the time-dependent

TABLE 1. The constant equilibria that are always solutions of the system of differential equations (7a, b).

| $\hat{p}_1(x)$ | $\hat{p}_2(x)$ | Biological interpretation |
|---|---|---|
| 0 | 0 | fixation of matching alleles |
| 1 | 1 | fixation of matching alleles |
| 0 | 1 | fixation of alternative alleles |
| 1 | 0 | fixation of alternative alleles |
| ½ | ½ | fully polymorphic |

partial differential equations (6) to analyze the approximate dynamics of geographically structured coevolutionary interactions.

## RESULTS

### *Antagonistic Coevolution*

We first consider a geographically structured coevolutionary interaction between a host and parasite, where the parasite always benefits from the interaction ($c_i$ or $c(x) > 0$ for all $i$ or $x$), and the host always suffers ($b_i$ or $b(x) < 0$ for all $i$ or $x$). We investigate interactions with spatially homogeneous selection (i.e., constant parasite virulence) and then those with spatially heterogeneous selection (i.e., spatial variation in parasite virulence). Although most interactions are unlikely to be subject to truly homogeneous reciprocal selection across large geographic regions, investigating this case provides a baseline expectation for the minimum role that coevolution may play in shaping patterns of clinal variation in interacting species.

If fitnesses are homogeneous across the geographic range of a host-parasite interaction, clines can only evolve when there is initial spatial heterogeneity in allele frequencies. In the absence of initial heterogeneity, equations (6) predict local oscillations in allele frequencies that are completely synchronized throughout the entire range of the interaction, producing allele frequencies that are constant across space, although dynamic through time (Gavrilets and Hastings 1998). When initial allele frequencies are heterogeneous, numerical simulation of the discrete time and space recursion equations (1)–(4) indicates that oscillations will be initially asynchronous across the range of the interaction, producing transient clines that change in shape through time, but eventually decay (Fig. 3A–F). These transient clines may lead to alternating patterns of local maladaptation (average fitness lower within sympatric than allopatric interactions) and local adaptation (average fitness higher within sympatric than allopatric interactions) within both interacting species as the spatial structure of allele frequencies changes through time (Fig. 3A–C). Furthermore, individuals drawn from any spe-

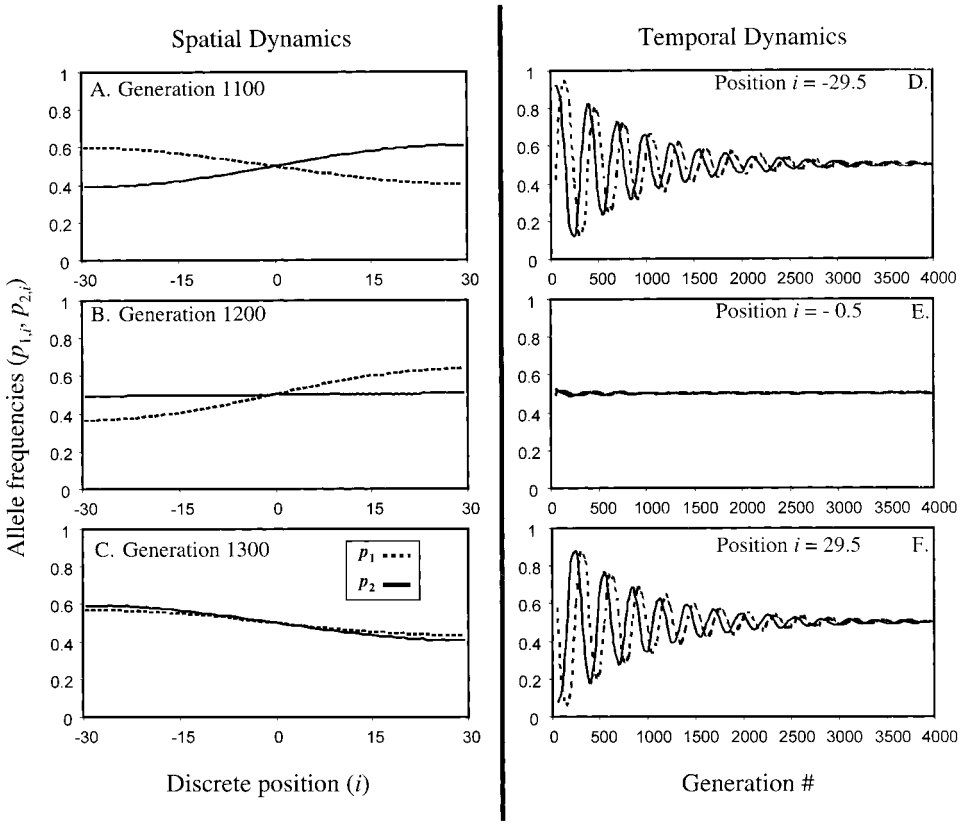


FIG. 3. Spatial and temporal structure of a dynamic cline within an antagonistic interaction. Panels (A), (B), and (C) show the geographic structure of allele frequencies $p_{1,i}$ and $p_{2,i}$ at generations 1100, 1200, and 1300 respectively; (D), (E), and (F) show the temporal dynamics of allele frequencies at three discrete locations $i = -29.5$, $i = -0.5$, and $i = 29.5$. These dynamics result from numerical simulation of equation (3), with $b_i = -0.04$, $c_i = 0.05$, $\sigma_1 = \sigma_2 = 1$, and $n = 60$. Initial allele frequencies were $p_{1,i} = 0.1$ for $\{-29.5 < i < 0\}$, $p_{1,i} = 0.9$ for $\{0 < i < 29.5\}$, $p_{2,i} = 0.8$ for $\{-29.5 < i < 0\}$, $p_{2,i} = 0.2$ for $\{0 < i < 29.5\}$. This initial spatial heterogeneity in allele frequencies has virtually disappeared by generation 4000.

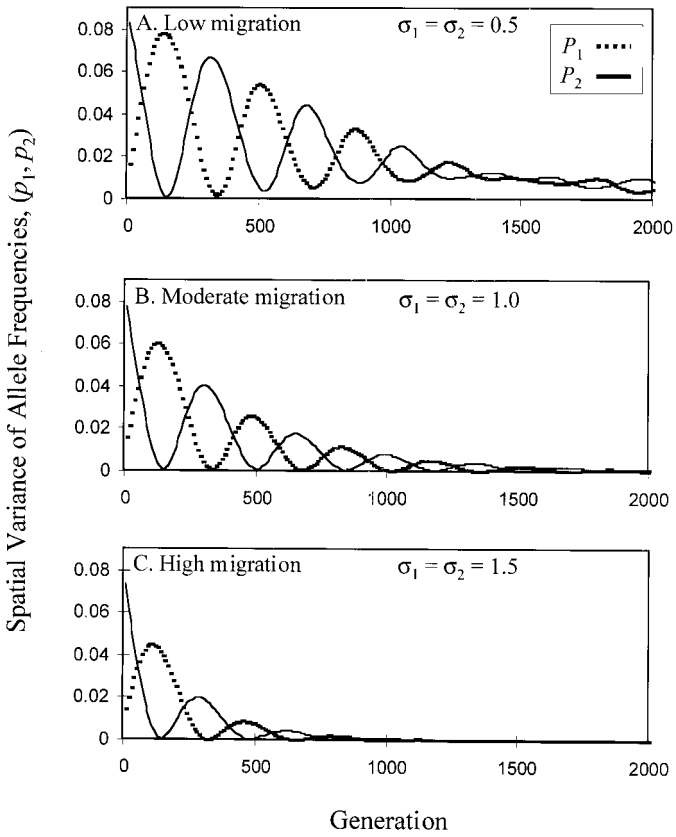


FIG. 4. The decay of spatial variance in allele frequencies $p_1$ and $p_2$ with time, showing the dependence of the rate of decay on the migration rates of interacting species. The spatial variance was calculated as $V(p_k) = \Sigma_{i=1}^{n} (p_{k,i} - \bar{p}_k)^2/(n - 1)$ from a numerical simulation of equation (3) with $c_i = 0.02$, $b_i = -0.02$,, $n = 70$. Initial allele frequencies were $p_{1,i} = 0.4$, $p_{2,i} = 0.3$ for $\{-34.5 < i < 0\}$ and $p_{1,i} = 0.6$, $p_{2,i} = 0.9$ for $\{0 < i < 34.5\}$. Migration rates were (A) $\sigma_1 = \sigma_2 = 0.5$; (B) $\sigma_1 = \sigma_2 = 1$; (C) $\sigma_1 = \sigma_2 = 1.5$.

cific geographic location *i* may be locally maladapted relative to individuals in one direction, while locally adapted to individuals in the other direction (Fig. 3).

Because the shape of transient clines at any instant depends strongly on initial conditions, spatially structured antagonistic interactions without selection mosaics are unlikely to produce predictable patterns of local maladaptation at any given moment in time. Furthermore, numerical simulation of the discrete model indicates that gene flow will eventually synchronize oscillations, leading to the decay of transient clines and the loss of spatially structured adaptation or maladaptation. The rate at which spatial variation decays depends primarily upon the rate of gene flow, with increasing gene flow leading to more rapid homogenization of allele frequencies (Fig. 4). Because transient clines are inevitably eroded by gene flow, coevolutionary clines will persist only for limited periods of time in the absence of selection mosaics.

By incorporating a selection mosaic ($b_L \neq b_R$ and/or $c_L \neq c_R$), such as geographic variation in parasite virulence (Fig. 2A), dynamic clines can evolve from allele frequencies that are initially homogenous across space. Furthermore, the incorporation of a selection mosaic on one species allows clines in both species to be permanently maintained under a restrictive set of conditions. Numerical simulation of the discrete model indicates that dynamic clines are most likely to arise and persist when both host and parasite have very low levels of gene flow relative to the width of the habitat (i.e., $A + B \gg \sigma_k$), and both species have strong reciprocal effects on fitness. These conditions allow temporal oscillations in allele frequencies to remain permanently asynchronous, thus creating clines that change shape rapidly through time (qualitatively similar to Fig. 3). When gene flow is high relative to the total width of habitat and the magnitude of reciprocal selection, allelic oscillations within both species converge to the fully polymorphic and geographically uniform equilibrium ($\hat{p}_{1,i} = \hat{p}_{2,i} = 1/2$). This fully polymorphic equilibrium represents a compromise condition where the fitness of both species is exactly half its maximum value throughout the habitat. When gene flow becomes very high relative to both the width of the habitat (e.g., $A + B < \sigma_k$) and the magnitude of reciprocal selection, allele frequency oscillations synchronize and increase in amplitude throughout the habitat. As intuition would predict, this case rapidly leads to the spatial homogenization of allele frequencies and the concomitant loss of spatial patterns of local maladaptation or adaptation. Together, these results demonstrate that spatial patterns of local maladaptation or adaptation are most likely to be permanently maintained in interactions characterized by very low rates of gene flow and strong, spatially heterogeneous reciprocal selection.

### *Mutualistic Coevolution*

We next consider a mutualistic interaction between a symbiont and host, where throughout their geographic ranges both species benefit from interacting ($c_i$, $b_i$ or $c(x)$, $b(x) > 0$ for all $i$ or $x$). We use the model to first investigate geographically structured mutualistic coevolution in the absence of a selection mosaic, where both interacting species affect each other equally throughout the habitat. We then introduce a selection mosaic, where mutualistic selection is stronger within some portions of the geographic range of the interaction than in others (Fig. 2B). Numerical simulation of the discrete equations (1)–(4) shows that both conditions lead to equilibria rather than to the temporal oscillations produced by spatially structured antagonistic coevolution. Whether these equilibria occur as clines or fixed monomorphisms depends on the relative strengths of selection and gene flow, the width of habitat, and the initial distribution of allele frequencies.

First, consider the case where selection is mutualistic and spatially homogenous throughout the range of the interaction. Analysis of both the discrete and continuous models shows that polymorphic clines tend to evolve when gene flow is low relative to the total width of habitat ($A + B$), and to the strength of reciprocal selection. These properties emerge readily from equilibrium equations (7) and from simulations of the discrete model (eqs. 1–4). If both interacting species have identical ratios of selection intensity to gene flow ($\omega_1(x) = \omega_2(x) = \omega$), then for any polymorphic equilibria the frequencies $\hat{p}_1(x)$ and $\hat{p}_2(x)$ must also be equal. Equations (7a,b) then collapse to a single equation:

$$\frac{d^2\hat{p}(x)}{dx^2} = -\omega\hat{p}(1-\hat{p})(2\hat{p}-1), \qquad \{-A < x < B\} \quad (8)$$

where $\hat{p}(x) = \hat{p}_1(x) = \hat{p}_2(x)$ . Equation (8) also arises in models of single-species clines maintained by selection against hybrids, and was originally formulated by Bazykin (1969) for this purpose. This strong parallel between clines maintained by mutualistic coevolution and clines maintained by selection against hybrids reflects the inherent instability of polymorphic equilibria within single populations for both types of selection. With the assumption that the interaction occurs across an infinite environment ($A = B = \infty$), equation (8) with boundary conditions

$$\frac{d\hat{p}}{dx} = 0 \quad \text{as } x \to \infty \quad \text{and} \quad \hat{p}(x) \to 1 \text{ or } 0 \qquad (9a)$$

and

$$\frac{d\hat{p}}{dx} = 0 \quad \text{as } x \to -\infty \quad \text{and} \quad \hat{p}(x) \to 0 \text{ or } 1 \qquad (9b)$$

can be solved, giving the spatially uniform monomorphic solutions of Table 1. There are also an infinite number of polymorphic clines, each centered at the arbitrary point $x_0$. These clines take one of two possible shapes given by the solutions:

$$\hat{p}(x) = \frac{1}{1 + \exp[(x - x_0)\sqrt{\omega}]} \quad \text{and} \qquad (10a)$$

$$\hat{p}(x) = \frac{\exp[(x - x_0)\sqrt{\omega}]}{1 + \exp[(x - x_0)\sqrt{\omega}]}, \qquad (10b)$$

which correspond to the two alternative boundary conditions given above. The presence of alternative solutions for each arbitrary value of $x_0$ suggests that the equilibrium shape of clines may be sensitive to initial allele frequencies. This suggestion is verified by numerical simulation of the discrete model with finite habitats ($n < \infty$). If initial allele frequencies are spatially uniform, fixed matching monomorphisms result rather than polymorphic clines. Because clines require initial spatial structuring of allele frequencies, they may be most likely to evolve in natural populations when genetic divergence has previously occurred in allopatry.

Once polymorphic clines have evolved within a geographically structured mutualism, their persistence is greatly enhanced by gene flow that is low relative to the total width of habitat. Numerical simulation of the discrete model suggests that the polymorphic equilibria described by equations (10) are much more stable to perturbations when the width of the habitat ($A + B$) exceeds the total width of the polymorphic cline estimated below. Extrapolating linearly from the maximum slope of the clines described by equations (10) estimates the width of these clines as

$$W = \frac{4}{\sqrt{\omega}}, \qquad (11)$$

which is analogous to Slatkin's (1973) ''characteristic length.'' Because habitats wider than $W$ promote stability (i.e., $A + B \gg W$), clines are most likely to persist within mutualistic interactions when gene flow is low relative to habitat width and the strength of reciprocal selection. Although these conclusions apply only to the simplified case where $\omega_1(x) = \omega_2(x) = \omega$, and the environment is infinite, numerical simulation of the discrete model suggests that our results are in good qualitative agreement with the more general condition ($\omega_1 \neq \omega_2$) if the restricted $\omega$ is assigned the smaller of the values $\omega_1$ or $\omega_2$.

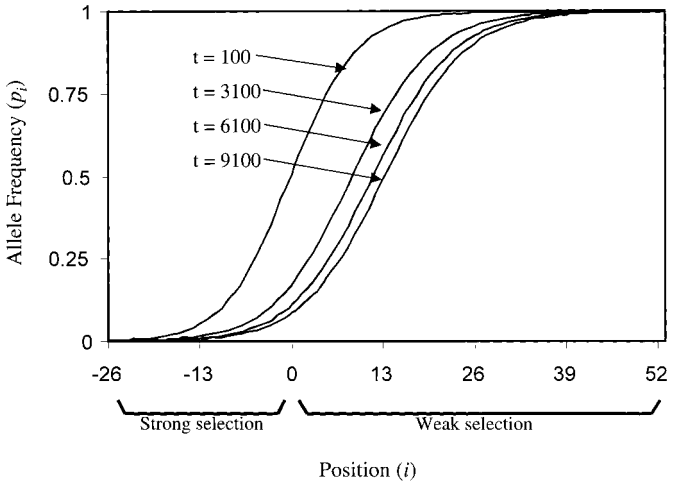


FIG. 5. The displacement of polymorphic cline from a region of strong mutualistic selection $\{-25.5 < i < 0\}$, into a region of weak mutualistic selection $\{0 < i < 51.5\}$. The four lines show the cline at generations 100, 3100, 6100, 9100. Results are from a numerical simulation of equation (3), with $b_L = 0.02$, $b_R = 0.15$, $c_L = 0.02$, $c_R = 0.015$, and $\sigma_1 = \sigma_2 = 1$.

Perhaps surprisingly, selection mosaics tend to limit the conditions that allow clines to evolve and be maintained within geographically structured mutualisms. When a selection mosaic exists within a mutualistic interaction such that $c_L \neq c_R$ and/or $b_L \neq b_R$, equilibrium equations (7) can be written as:

$$\frac{d^2\hat{p}_1}{dx^2} = \begin{cases} -\omega_1\hat{p}_1(1-\hat{p}_1)(2\hat{p}_2-1) & \{-A < x < 0\} \\ -\alpha_1\omega_1\hat{p}_1(1-\hat{p}_1)(2\hat{p}_2-1) & \{0 < x < B\} \end{cases} \qquad (12a)$$

and

$$\frac{d^2\hat{p}_2}{dx^2} = \begin{cases} -\omega_2\hat{p}_2(1-\hat{p}_2)(2\hat{p}_1-1) & \{-A < x < 0\} \\ -\alpha_2\omega_2\hat{p}_2(1-\hat{p}_2)(2\hat{p}_1-1), & \{0 < x < B\} \end{cases} \qquad (12b)$$

where $\alpha_1 = |c_R/c_L|$, $\alpha_2 = |b_R/b_L|$, $\omega_1 = |2c_L/l_1^2|$, and $\omega_2 = |2b_L/l_2^2|$. If we again assume an infinite habitat ($A = B = \infty$) and $\omega_1 = \omega_2 = \omega$, analysis of equations (12) reveals that clines cannot be polymorphic as they cross the boundary of the selection mosaic, at $x = 0$ (Appendix 1A). That is, both species must be monomorphic at the border between regions of differing selection intensities. This analytic result is corroborated by numerical simulations of the discrete model with finite habitats. In general, the incorporation of selection mosaics results in the displacement of clines from the region of stronger mutualistic selection (Fig. 5). Habitat width, in relation to the compound parameter $\omega$, determines whether this displacement leads to the loss of a polymorphic cline through-

out the habitat or simply causes it to be displaced from the region of stronger selection. The critical width of habitat necessary to maintain the polymorphic cline in the presence of a selection mosaic can be estimated as

$$B > \frac{4}{\sqrt{\omega}}, \tag{13}$$

where $B$ is the width of the habitat in which reciprocal selection is weaker (Appendix 1B). This condition demonstrates that elimination of a polymorphic cline is independent of the strength of selection within the more strongly selected habitat. When a selection mosaic displaces a cline, the distance the cline will shift from the selection mosaic boundary is approximately equal to half the width of habitat required to maintain the cline, or $2/\sqrt{\omega}$. This value is independent of the ratio of reciprocal selection within the two regions, with the distance the polymorphic cline travels being determined solely by the amount of gene flow and strength of reciprocal selection within the less strongly selected region. Numerical simulation of the discrete model suggests that these results are valid even for the more general condition ($\omega_1 \neq \omega_2$), if $\omega$ is assigned the smaller of the values $\omega_1$ or $\omega_2$. Taken together, these results show that clines are most likely to exist within geographically structured mutualisms when reciprocal selection is strong, gene flow is low relative to the width of habitat, and selection mosaics are absent ($\alpha_1 = \alpha_2 = 1$).

### *Selection Mosaic between Mutualism and Antagonism*

Finally, we consider an interaction between a symbiont and host that varies geographically from antagonism to mutualism (Fig. 2C). Such interactions may frequently occur within mutualisms when the relative costs and benefits of the interaction change with differences in local ecological conditions (Barton 1986; Cushman and Whitham 1989; Thompson and Pellmyr 1992; Breton and Addicot 1992; Saikkonen et al. 1998). When ecological conditions vary through space such that selection varies between antagonism and mutualism, the results described in this section show that both dynamic and equilibrium clines are common.

We first consider a simplified case where the symbiont species is monomorphic ($p_1(x) = 0$ or 1), perhaps through abiotic or biotic factors extrinsic to the interaction. In this case, polymorphic clines readily evolve within the host. If selection is antagonistic ($c_L > 0$, $b_L < 0$) within the geographic region $\{-A < x < 0\}$ but mutualistic ($c_R$, $b_R > 0$) within the alternative region $\{0 < x < B\}$, equilibrium equations (7) reduce to

$$\frac{d^2\hat{p}_2}{dx^2} = \begin{cases} \mp\omega_2\hat{p}_2(1 - \hat{p}_2) & \{-A < x < 0\} \\ \pm\alpha_2\omega_2\hat{p}_2(1 - \hat{p}_2), & \{0 < x < B\} \end{cases} \tag{14}$$

where $\alpha_2 = |b_R/b_L|$, and $\omega_2 = |2b_L/l_2^2|$. The upper signs apply when the symbiont is fixed for the y allele ($\hat{p}_1(x) \equiv 0$) whereas the lower signs apply when the symbiont is fixed for the Y allele ($\hat{p}_1(x) \equiv 1$). Equation (14) also determines the equilibrium allele frequencies for a single species evolving across an environmental step cline (Haldane 1948; Slatkin 1973). When the magnitude of selection on the host is equal between regions of antagonism and mutualism ($\alpha_2 = 1$) and the environment is infinite ($A = B = \infty$), equations (14) subject to the boundary conditions

$$\frac{d\hat{p}_2}{dx} = \begin{cases} 0 & x \to \infty \quad \hat{p}_2(x) \to 0 \\ 0 & x \to -\infty \quad \hat{p}_2(x) \to 1 \end{cases} \tag{15a}$$

for $\hat{p}_1(x) \equiv 0$ and

$$\frac{d\hat{p}_2}{dx} = \begin{cases} 0 & x \to \infty \quad \hat{p}_2(x) \to 1 \\ 0 & x \to -\infty \quad \hat{p}_2(x) \to 0 \end{cases} \tag{15b}$$

for $\hat{p}_1(x) \equiv 1$ can be solved, giving

$$\hat{p}_2(x) = \begin{cases} -\frac{1}{2} + \frac{3}{2}\tanh\left(\operatorname{arctanh}\sqrt{2/3} - \frac{\sqrt{\omega_2}}{2}x\right)^2 \\ \qquad \{-\infty < x < 0\} \\ \frac{3}{2} - \frac{3}{2}\tanh\left(\operatorname{arctanh}\sqrt{2/3} + \frac{\sqrt{\omega_2}}{2}x\right)^2 \\ \qquad \{0 < x < \infty\}, \end{cases} \tag{16a}$$

if $\hat{p}_1(x) \equiv 0$, and

$$\hat{p}_2(x) = \begin{cases} \frac{3}{2} - \frac{3}{2}\tanh\left(\operatorname{arctanh}\sqrt{2/3} - \frac{\sqrt{\omega_2}}{2}x\right)^2 \\ \qquad \{-\infty < x < 0\} \\ -\frac{1}{2} + \frac{3}{2}\tanh\left(\operatorname{arctanh}\sqrt{2/3} + \frac{\sqrt{\omega_2}}{2}x\right)^2 \\ \qquad \{0 < x < \infty\}, \end{cases} \tag{16b}$$

if $\hat{p}_1(x) \equiv 1$. Solutions (16) describe polymorphic clines in the host and demonstrate that the spatial structure of adaptation will differ for host and symbiont species (Fig. 6). Minimum host fitness occurs at the mutualism-antagonism interface ($x = 0$), whereas symbiont fitness reaches its minimum within the region of antagonistic reciprocal selection.

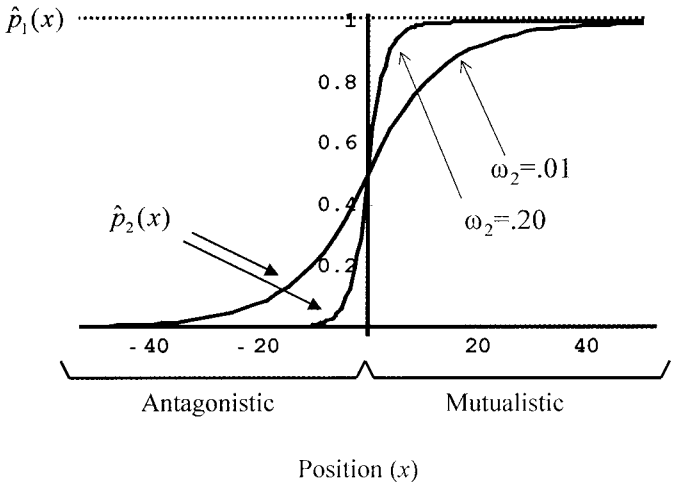


FIG. 6. Two plots of the equilibrium allele frequency of the host species, $\hat{p}_2(x)$, for selection that varies between antagonism within the region $\{-\infty < x < 0\}$ and mutualism within the region $\{0 < x < \infty\}$. The allele frequency of the symbiont species is fixed at $\hat{p}_1(x) = 1$ throughout the range of the interaction. Results are from equation (16b), with $\omega_2 = 0.20$ and 0.01 respectively.

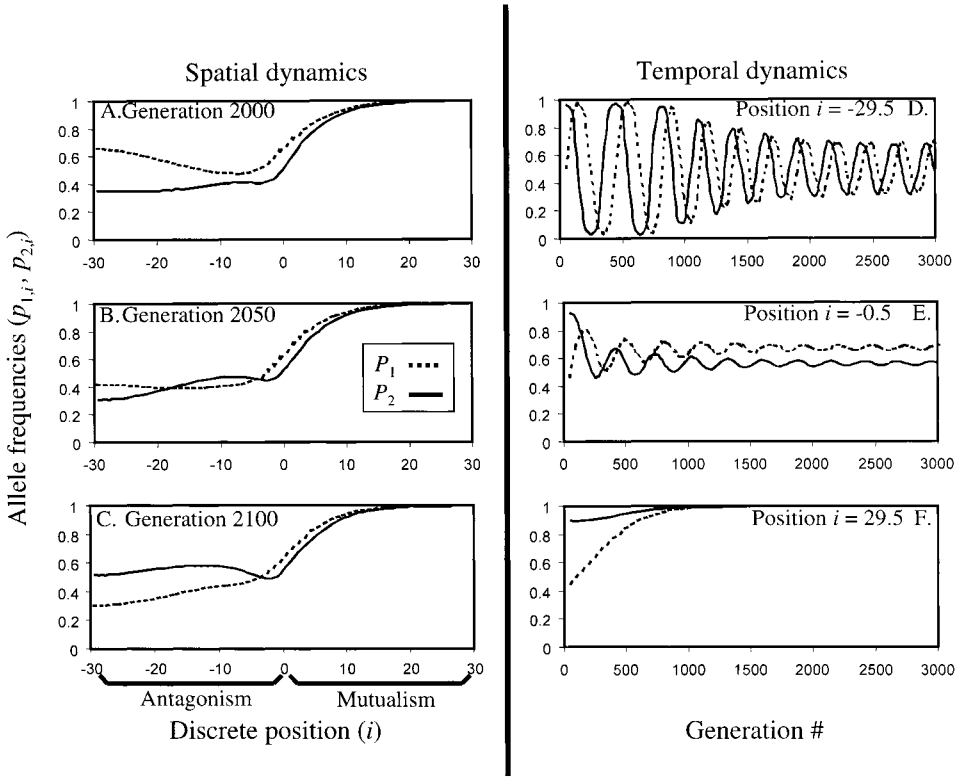


FIG. 7. A dynamic cline within an interaction that varies between antagonism and mutualism. Panels (A), (B), and (C) show the geographic structure of allele frequencies $p_1$ and $p_2$ at generations 2000, 2050, and 2100, respectively; (D), (E) and (F) show the temporal dynamics of allele frequencies at three discrete locations $i = -29.5$, $i = -0.5$ and $i = 29.5$. These dynamics results from numerical simulation of equation (3) across a step cline where $b_L = -0.05$, and $c_L = 0.05$ within the antagonistic region $\{-29.5 < i < 0\}$ and $c_R = 0.05$ and $b_R = 0.05$ within the mutualistic region $\{0 < i < 29.5\}$, $\sigma_1 = \sigma_2 = 0.5$, and $n = 60$. Initial allele frequencies were $p_{1,i} = 0.1$, $p_{2,i} = 0.9$ for $\{-29.5 < i < 0\}$ and $p_{1,i} = 0.4$, $p_{2,i} = 0.9$ for $\{0 < i < 29.5\}$.

Furthermore, the width of habitat over which hosts fail to maximize fitness is given by $\sqrt{6/\omega_2}$, indicating that this region of maladaptation increases with host gene flow and decreases with the intensity of reciprocal selection.

When both species are free to evolve, numerical simulations of the discrete model indicate that equilibrium clines and temporally dynamic clines will both evolve within linked antagonistic-mutualistic systems. Dynamic clines are restricted to conditions of very low gene flow relative to the width of antagonistic habitat or antagonistic selection that is much stronger than mutualistic selection. This result must clearly be true in the limit as the region of antagonistic selection becomes very large relative to gene flow and local reciprocal selection predominates, leading to oscillations within at least some portion of the antagonistic habitat. A common result from simulations is oscillatory temporal dynamics within the antagonistic habitat that decrease in amplitude with proximity to the region of mutualistic selection (Fig. 7). Within the mutualistic region, these temporally dynamic oscillations are gradually replaced by the matched monomorphic equilibrium (Fig. 7). Overall, these conditions tend to limit oscillations within antagonistic habitats and prevent monomorphic fixation within mutualistic habitats, promoting the maintenance of polymorphism across the range of the interaction.

When gene flow is high relative to the width of the antagonistic habitat and the region of mutualism is much larger or more strongly selected than the region of antagonism, stable equilibrium clines predominate. These clines are highly polymorphic within antagonistic habitats, with levels of polymorphism decreasing and eventually being replaced by fixed monomorphisms as distance from the antagonism-mutualism boundary increases (Fig. 8). These equilibrium clines lead to strong spatial patterns of maladaptation, with the mean fitness of both species being furthest from its potential maximum within the antagonistic habitat. As distance from the antagonistic habitat increases, levels of maladaptation generally decrease within both interacting species as allele frequencies approach a fixed monomorphic equilibria with optimal fitness for both species, within the mutualistic habitat.

For studies of evolving mutualisms, the conditions necessary to replace both dynamic and equilibrium clines with fixed matching monomorphisms ($\hat{p}_1(x) = \hat{p}_2(x) = 0$ or 1) are of particular interest. These matching monomorphisms correspond to fixed mutualisms, where both species are fixed for matching alleles and therefore, by assumption, always successfully interact. The conditions that allow these fixed mutualisms to be evolutionarily stable in the face of pockets of locally antagonistic selection are of fundamental importance to understanding the conditions that favor the evolution of obligate mutualisms, such as those between figs and fig wasps and yuccas and yucca moths. When an interaction varies geographically between antagonism and mutualism,

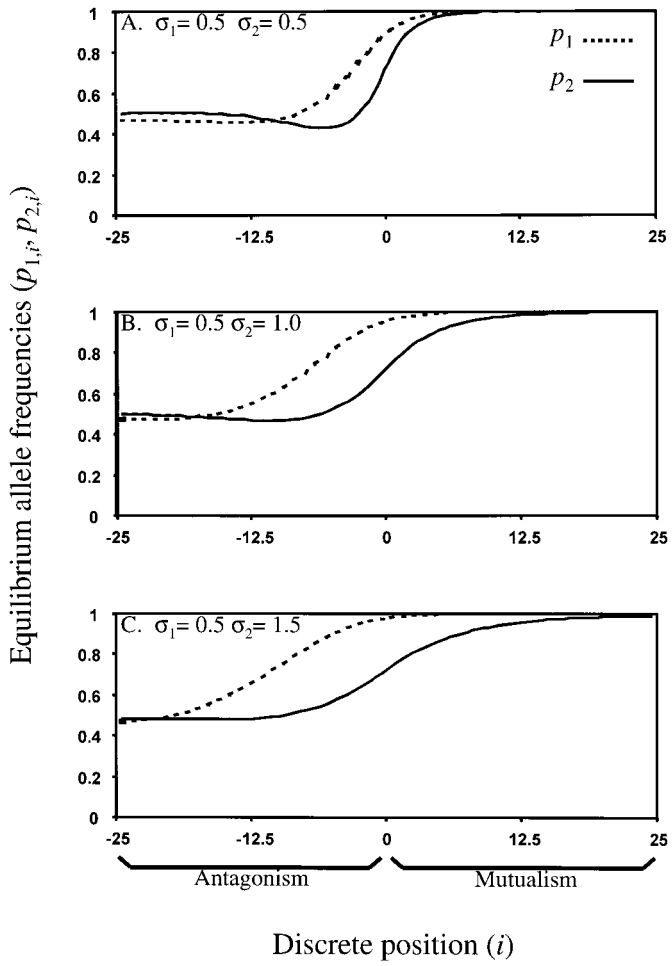


FIG. 8. An equilibrium cline within an interaction that varies between antagonism and mutualism, showing the geographic structure of the equilibrium allele frequencies $\hat{p}_{1,i}$ and $\hat{p}_{2,i}$ for different host migration rates $\sigma_2$. Plots result from numerical simulation of equation (3) across a step cline where $b_L = -0.02$, and $c_L = 0.03$ within the antagonistic region $\{-24.5 < i < 0\}$, and $c_R = 0.03$ and $b_R = 0.03$ within the mutualistic region $\{0 < i < 24.5\}$, and $n = 50$. Migration rates of the symbiont/parasite were fixed with $\sigma_1 = 0.5$, while host migration rates were: (A) $\sigma_2 = 0.5$; (B) $\sigma_2 = 1.0$; and (C) $\sigma_2 = 1.5$. Initial allele frequencies were $p_{1,i} = 0.3$, $p_{2,i} = 0.8$ for $\{-24.5 < i < 0\}$ and $p_{1,i} = 0.4$, $p_{2,i} = 0.8$ for $\{0 < i < 24.5\}$.

analysis of equations (6) (Appendix 2) reveals that a sufficient condition for the stability of the matching monomorphic equilibria is

$$\omega_2 A^2 < \theta_0 \tag{17a}$$

where $\omega_2 = |2b_L/l_2^2|$, and $\theta_0$ is the unique root between 0 and $\pi/2$ of

$$\tan(\sqrt{\theta_0}) = \sqrt{\alpha_2}\tanh(\gamma\sqrt{\theta_0\alpha_2}), \tag{17b}$$

with $\gamma = B/A$, and $\alpha_2 = |b_R/b_L|$.

This result demonstrates that the stability of fixed mutualisms depends directly on host parameters alone. Moreover, equations (17) are identical to the stability condition for a single species evolving within a spatially heterogeneous environment derived by (Nagylaki 1975). Equation (17a) also suggests that the balance between host gene flow and selection exerted by the symbiont (reflected in $\omega_2$) is of crucial importance in determining the appropriate scale of empirical investigation.

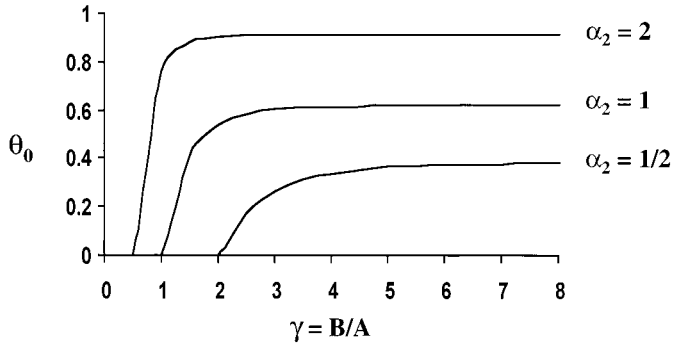


FIG. 9. The critical value $\theta_0$ calculated from equation (17b) and plotted against $\gamma$, the ratio of the sizes of mutualistic (B) to antagonistic (A) habitat, for three different values of $\alpha_2$. For the fixed mutualism to be stable, $\omega_2 A^2 < \theta_0$. The figure shows that increasing the strength of mutualistic selection relative to antagonistic selection, $\alpha_2$, increases the range of parameters capable of maintaining a fixed mutualism. The plot also shows that as the ratio of mutualistic to antagonistic habitat, $\gamma$, increases, the critical value, $\theta_0$ increases rapidly and then plateaus.

Finally, increasing the ratio of mutualistic to antagonistic habitat, $\gamma$, causes the critical value $\theta_0$ to increase, with this increase occurring rapidly and over only a very small region of $\gamma$ (Fig. 9). This abrupt relationship between $\gamma$ and $\theta_0$ indicates that changes in the relative proportions of mutualistic and antagonistic habitats will generally have very little impact on stability unless they occur within a critical region of host selection and gene flow. This result has clear implications for the conservation of species interactions and overall community structure, showing that very small changes in habitat size can dramatically restructure interspecific interactions.

## DISCUSSION

Our analyses suggest that geographically structured coevolution readily leads to both equilibrium and dynamic clines, thus potentially producing strong spatial structuring in the traits of interacting species. Both dynamic and equilibrium clines may evolve and persist in the presence of selection mosaics and, surprisingly, even in their absence. Whether clines arise and persist and are equilibrium or dynamic depends on the type of underlying coevolutionary selection as well as habitat size, rates of gene flow, and the strength of reciprocal selection.

The three types of geographically structured coevolution considered here lead to fundamentally different types of clines. In purely antagonistic interactions equilibrium clines do not evolve, but dynamic clines evolve readily when allele frequency oscillations are not synchronized throughout the geographic range of the interaction. Such dynamic spatial patterns are well known for a variety of biological, physical, and chemical systems that exhibit oscillatory behavior in the absence of spatial structuring (Murray 1993). Incorporating a selection mosaic into these antagonistic interactions allows dynamic clines to be generated de novo and promotes their

persistence. Unlike antagonistic interactions, geographically structured mutualisms tend to evolve stable equilibrium clines, with selection mosaics decreasing the likelihood that clines will evolve and persist. When coevolutionary selection varies from mutualism to antagonism across space, both dynamic and equilibrium clines are produced. These overall patterns depend on rates of gene flow, the relative strengths of coevolutionary selection between the mutualistic and antagonistic habitats, and the relative sizes of these two habitat types.

Our analysis of purely antagonistic interactions also suggests that dynamic clines will generally persist only when coevolutionary selection is strong and gene flow is weak relative to habitat width. When the opposite conditions prevail, dynamic clines decay at a rate that increases with increasing levels of gene flow. These results suggest that spatially structured patterns of adaptation or maladaptation are most likely in those coevolutionary systems characterized by strong and spatially variable reciprocal selection and gene flow that is weak relative to habitat width. These conditions are similar to those of Lively (1999), who used a two-patch coevolutionary model to investigate patterns of local adaptation in a parasite. This model showed that significant levels of local adaptation or maladaptation could only be maintained with low rates of parasite gene flow in conjunction with very high levels of parasite virulence. Furthermore, our results show that these spatial patterns of local adaptation will vary through time, with any population alternating between local adaptation and local maladaptation. Consequently, measures of local adaptation or maladaptation taken at only a single instant in time, rather than as time averages, may be very misleading.

These conditions lead to two general predictions about the spatial structure of local adaptation and maladaptation. First, because conditions of low gene flow and strong selection reduce the geographic scale over which gene frequencies correlate, we expect patterns of local adaptation or maladaptation to vary predictably only over a finite region. This prediction receives at least some support from empirical studies demonstrating correlations between geographic distance and local adaptation only over small spatial scales (Lively 1989; Wilkinson et al. 1996; Kaltz et al. 1999). Second, the distance over which correlations between local adaptation and geographic distance occur will be determined by the amount of gene flow, relative to the strength of reciprocal selection. Because this distance must be measured relative to rates of gene flow and the strength of reciprocal selection, different taxa may show patterns of local adaptation or maladaptation over markedly different spatial scales. This may partially explain why some empirical studies have not found evidence for local adaptation or maladaptation (Parker 1989; Ebert et al. 1998; Imhoof and Schmid-Hempel 1998), whereas other studies using different taxa or spatial scales have found such evidence (Parker 1985; Ballabeni and Ward 1993; Hanks and Denno 1994; Lively and Jokela 1996).

Our analyses also demonstrate that polymorphic clines can be maintained within mutualistic interactions. Of crucial importance to the persistence of clines is the relationship between gene flow, selection, and habitat size. Our analyses of geographically structured mutualisms suggest that clines are most likely to be maintained when the total habitat width in which the interaction occurs is much greater than $4/\sqrt{\omega}$. This result shows that the size of habitat required to maintain a cline decreases with higher intensities of coevolutionary selection, but increases with higher rates of gene flow. These results are in broad agreement with the results of a recent metapopulation model of geographically structured mutualisms (Parker 1999). Using a spatially explicit model, Parker's simulations showed that polymorphic patterns may be most likely to be maintained within mutualistic interactions when gene flow is low. Together, these results help to explain how mutualistic interactions may maintain polymorphisms on a geographic scale, despite local selection that favors matching monomorphisms.

Finally, our results show that fixed mutualisms, where both species successfully interact throughout their geographic ranges, may persist between species despite pockets of locally antagonistic selection. This result adds to the emerging view that mutualisms may be demographically and genetically more stable than previously thought (Pellmyr and Huth 1994; Pellmyr et al. 1996; Ringel et al. 1996). Furthermore, our results show that, although fixed mutualisms may be stable across a broad range of parameter values, a critical region exists where even small changes in the proportions of mutualistic and antagonistic habitats may destabilize the mutualism and lead to a restructuring of overall community dynamics.

The model we have considered is relatively simple, but the results show that geographic structure may produce coevolutionary dynamics that are impossible within local interactions. Investigation of more complex models that incorporate other aspects of geographically structured coevolution, such as spatial variation in ecological dynamics or interactions that vary between regions of coevolutionary selection (hot spots) and commensalistic selection (cold spots) may expand upon the results of our simple model (e.g., Gomulkiewicz et al. 2000). Likewise, the incorporation of more complex genetic systems may allow novel coevolutionary dynamics to emerge as epistatic interactions among loci are reshaped by selection, gene flow, and drift. Consideration of these additional complexities will be necessary for a more complete understanding of the causes and consequences of geographically structured coevolution.

## Acknowledgments

We thank K. Merg, B. Cunningham, M. Hochberg, B. Holt, and S. Otto for helpful discussions of this work and T. Day for insightful advice on analyses. We also thank S. Gandon and S. Gavrilets for very helpful comments on the manuscript. This work was supported by National Science Foundation grant DEB-9707781 to JNT, National Science Foundation grant DEB-9528602 to RG, and by the National Center for Ecological Analysis and Synthesis (Coevolution Working Group) National Science Foundation grant DEB-9421535.

## Literature Cited

Ballabeni, P., and P. I. Ward. 1993. Local adaptation of the trematode *Diplostomum phoxini* to the European minnow *Phoxinus*, its second intermediate host. Functional Ecology 7:84–90.

Barton, A. 1986. Spatial variation in the effect of ants on an extrafloral nectary plant. Ecology 67:495–504.
Barton, N. H. 1979. The dynamics of hybrid zones. Heredity 43: 341–359.
———. 1983. Multilocus clines. Evolution 87:454–471.
———. 1999. Clines in polygenic traits. Genet. Res. 74:223–236.
Barton, N. H., and G. M. Hewitt. 1985. Analysis of hybrid zones. Annu. Rev. Ecol. Syst. 16:113–148.
Bazykin, A. D. 1969. A hypothetical mechanism of speciation. Evolution 23:685–687.
Benkman, C. W. 1999. The selection mosaic and diversifying coevolution between crossbills and lodgepole pine. Am. Nat. 153: S75–S91.
Berenbaum, M. R., and A. R. Zangerl. 1998. Chemical phenotype matching between a plant and its insect herbivore. Proc. Natl. Acad. Sci. USA 95:13743–13748.
Breton, L. M., and J. F. Addicot. 1992. Density-dependent mutualism in an aphid-ant interaction. Ecology 73:2175–2180.
Brodie, E. D. III, and E. D. Brodie, Jr. 1999. Costs of exploiting poisonous prey: evolutionary trade-offs in a predator-prey arms race. Evolution 53:626–631.
Campbell, D. R., N. M. Waser, and E. J. Melendex-Ackerman. 1997. Analyzing pollinator-mediated selection in a plant hybrid zone: hummingbird visitation patterns on three spatial scales. Am. Nat 149:295–315.
Cushman, H. J., and T. G. Whitham. 1989. Conditional mutualism in a membracid-ant association: temporal, age-specific, and density-dependent effects. Ecology 70:1040–1047.
Ebert, D., C. D. Zschokke-Rohringer, and H. J. Carius. 1998. Within- and between- population variation for resistance of *Daphnia magna* to the bacterial endoparasite *Pasteuria ramosa.* Proc. R. Soc. Lond. B 265:2127–2134.
Endler, J. A. 1973. Gene flow and population differentiation. Science 179:243–250.
Fisher, R. A. 1937. The wave of advance of advantageous genes. Ann. Eugen. 7:355–369.
———. 1950. Gene frequencies in a cline determined by selection and diffusion. Biometrics 6:353–361.
Frank, S. A. 1993. Coevolutionary genetics of hosts and parasites with quantitative inheritance. Evolutionary ecology 7:1–21.
———. 1997. Spatial processes in host-parasite genetics. Pp. 325–352 *in* I. Hanski and M. E. Gilpen, eds. Metapopulation biology. Academic Press, San Diego, CA.
Gandon, S., Y. Capowiez, Y. Dubois, Y. Michalakis, and I. Olivieri. 1996. Local adaptation and gene-for-gene coevolution in a metapopulatiion model. Proc. R. Soc. Lond. B 263:1003–1009.
Garcia-Ramos, G., and M. Kirkpatrick. 1997. Genetic models of adaptation and gene flow in peripheral populations. Evolution 51:21–28.
Gavrilets, S. 1997. Single locus clines. Evolution 51:979–983.
Gavrilets, S., and A. Hastings. 1998. Coevolutionary chase in two-species systems with applications to mimicry. J. Theor. Biol. 191:415–427.
Gomulkiewicz, R., J. N. Thompson, R. D. Holt, S. L. Nuismer, and M. E. Hochberg. 2000. Hot spots, cold spots, and the geographic mosaic theory of coevolution. Am. Nat. 156: *In press.*
Haldane, J. B. S. 1948. The theory of a cline. J. Genet. 48:277–284.
Hanks, L. M., and R. F. Denno. 1994. Local adaptation in the armored scale insect *Pseudaulacaspis pentagona* (homoptera: diaspididae). Ecology 75:2301–2310.
Hochberg, M. E., and M. van Baalen. 1998. Antagonistic coevolution over productivity gradients. Am. Nat. 152:620–634.
Imhoof, B., and P. Schmid-Hempel. 1998. Patterns of local adaptation of a protozoan parasite to its bumblebee host. OIKOS 82: 59–65.
Kaltz, O., S. Gandon, Y. Michalakis, and J. A. Shykoff. 1999. Local maladaptation in the anther-smut fungus *Microbotryum violaceum* to its host plant *Silene latifolia:* evidence from a cross inoculation experiment. Evolution 53:395–407.
Kirkpatrick, M., and N. H. Barton. 1997. Evolution of a species range. Am. Nat. 150:1–23.
Kraaijeveld, A. R., and H. C. J. Godfray. 1999. Geographical patterns in the evolution of resistance and virulence in *Drosophila* and its parasitoids. Am. Nat. 153:S61–S74.
Kruuk, L. E. B., S. J. E. Baird, K. S. Gale, and N. H. Barton. 1999. A comparison of multilocus clines maintained by environmental adaptation or by selection against hybrids. Genetics 153: 1959–1971.
Leonard, K. J. 1997. Modeling gene frequency dynamics. Pp. 211–230 *in* I. R. Crute, E. B. Holub, and J. J. Burdon, eds. The gene-for-gene relationship in plant-parasite interactions. CAB International, Wallingford, U.K.
Li, W. H., and M. Nei. 1974. Stable linkage disequilibrium without epistasis in subdivided populations. Theor. Popul. Biol 6: 173–183.
Lively, C. M. 1989. Adaptation by a parasitic trematode to local populations of its snail host. Evolution 43:1663–1671.
———. 1999. The geographic mosaic of host-parasite coevolution: simulation models and evidence from a snail-trematode interaction. Am. Nat. 153:S34–S47.
Lively, C. M., and J. Jokela. 1996. Clinal variation for local adaptation in a host-parasite interaction. Proc. R. Soc. Lond. B 263:891–897.
Mallet, J., and N. Barton. 1989. Inferences from clines stabilized by frequency-dependent selection. Genetics 122:967–976.
Maschinski, J., and T. G. Whitham. 1989. The continuum of plant responses to herbivory: the influence of plant association, nutrient availability, and timing. Am. Nat. 134:1–19.
Michalakis, Y., I. Olivieri, F. Renaud, and M. Raymond. 1992. Pleiotropic action of parasites: how to be good for the host. TREE 7:59–62.
Munger, J. C., and J. C. Holmes. 1987. Benefits of parasitic infection: a test using the ground squirrel–trypanosome system. Can. J. Zool. 66:222–227.
Murray, J. D. 1993. Mathematical biology Springer-Verlag, New York.
Nagylaki, T. 1975. Conditions for the existence of clines. Genetics 80:595–615.
Nguyen, T. N. M., Q. G. Phan, L. P. Duong, K. P. Bertrand, and R. E. Lenski. 1989. Effects of carriage and expression of the Tn10 tetracycline-resistance operon on the fitness of *Escherichia coli* K12. Mol. Biol. Evol. 6:213–225.
Nuismer, S. L., J. N. Thompson, and R. Gomulkiewicz. 1999. Gene flow and geographically structured coevolution. Proc. R. Soc. Lond. B 266:605–609.
Parker, M. A. 1985. Local population differentiation for compatibility in an annual legume and its host-specific fungal pathogen. Evolution 39:713–723.
———. 1989. Disease impact and local genetic diversity in the clonal plant *Podophyllum peltatum.* Evolution 43:540–547.
———. 1999. Mutualism in metapopulations of legumes and rhizobium. Am. Nat. 153:S48–S60.
Pellmyr, O., and C. J. Huth. 1994. Evolutionary stability of mutualism between yuccas and yucca moths. Nature 372:257–260.
Pellmyr, O., J. Leebens Mack, and C. J. Huth. 1996. Non-mutualistic yucca moths and their evolutionary consequences. Nature 380: 155–156.
Ringel, M. S., H. H. Hu, and G. Anderson. 1996. The stability and persistence of mutualisms embedded in community interactions. Theoretical Population Biology 50:281–297.
Saikkonen, K., S. H. Faeth, M. Helander, and T. J. Sullivan. 1998. Fungal endophytes: a continuum of interactions with host plants. Annu. Rev. Ecol. Syst. 29:319–343.
Seger, J. 1988. Dynamics of some simple host-parasite models with more than two genotypes in each species. Phil. Trans. R. Soc. Lond. B 319:541–555.
Slatkin, M. 1973. Gene flow and selection in a cline. Genetics 75: 733–756.
———. 1975. Gene flow and selection in a two-locus system. Genetics 81:787–802.
Storfer, A., and A. Sih. 1998. Gene flow and ineffective antipredator behavior in a stream-breeding salamander. Evolution 52: 558–565.
Thompson, J. N. 1994. The coevolutionary process. Univ. of Chicago Press, Chicago.

———. 1999a. Specific hypotheses on the geographic mosaic of coevolution. Am. Nat. 153:S1–S14.
———. 1999b. The evolution of species interactions. Science 284: 2116–2118.
Thompson, J. N., and O. Pellmyr. 1992. Mutualism with pollinating seed parasites amid co-pollinators: constraints on specialization. Ecology 73:1780–1791.
Wilkinson, H. H., J. M. Spoerke, and M. A. Parker. 1996. Divergence in symbiotic compatibility in a legume-*Bradyrhizobium* mutualism. Evolution 50:1470–1477.

Corresponding Editor: D. Roff

## Appendix 1

Conditions for the existence of clines within spatially heterogeneous environments.

(A) Here we show that selection mosaics preclude the existence of clines that are polymorphic at the boundary ($x = 0$) of the selection mosaic. With the assumption that the interaction occurs in an infinite habitat ($A = B = \infty$) and that $\omega_1 = \omega_2 = \omega$, equations (12) become

$$\frac{d^2\hat{p}(x)}{dx^2} = -\omega\hat{p}(1 - \hat{p})(2\hat{p} - 1) \qquad \{-\infty < x < 0\} \quad \text{(A1)}$$

and

$$\frac{d^2\hat{p}(x)}{dx^2} = -\alpha\omega\hat{p}(1 - \hat{p})(2\hat{p} - 1), \qquad \{0 < x < \infty\} \quad \text{(A2)}$$

where $\alpha = |c_R/c_L| = |b_R/b_L|$, and $\hat{p}(x) = \hat{p}_1(x) = \hat{p}_2(x)$. Making the substitution $u = d\hat{p}/dx$, and solving (A1) and (A2) subject to the boundary conditions

$$\frac{d\hat{p}}{dx} = 0 \quad \text{and} \quad \hat{p} \to 0 \text{ or } 1 \quad \text{as } x \to -\infty, \quad \text{(A3)}$$

$$\frac{d\hat{p}}{dx} = 0 \quad \text{and} \quad \hat{p} \to 1 \text{ or } 0 \quad \text{as } x \to \infty, \quad \text{(A4)}$$

and

$$\hat{p}(x) \text{ is continuous at } x = 0. \quad \text{(A5)}$$

yields

$$\hat{p}(x) = \frac{-p_0}{-e^{x\sqrt{\omega}} + p_0(-1 + e^{x\sqrt{\omega}})} \qquad \{-\infty < x < 0\} \quad \text{(A6)}$$

and

$$\hat{p}(x) = \frac{-p_0}{-e^{x\sqrt{\alpha\omega}} + p_0(-1 + e^{x\sqrt{\alpha\omega}})}, \qquad \{0 < x < \infty\} \quad \text{(A7)}$$

where $p_0$ is an arbitrary value for $\hat{p}(x)$ at $x = 0$. Lastly, we require that $d\hat{p}(x)/dx$ be continuous at $x = 0$. Differentiating equations (A6) and (A7) with respect to x and evaluation at $x = 0$ yields

$$\frac{d\hat{p}}{dx} = (-1 + p_0)(p_0)\sqrt{\omega} \qquad \{-\infty < x < 0\} \quad \text{(A8)}$$

and

$$\frac{d\hat{p}}{dx} = (-1 + p_0)(p_0)\sqrt{\omega\alpha}, \qquad \{0 < x < \infty\} \quad \text{(A9)}$$

which can only be satisfied with $0 < p_0 < 1$ if $\alpha = 1$. Thus, polymorphic clines cannot exist across the boundary of regions of heterogeneous selection. (B) In the previous section we showed that selection mosaics do not allow clines that are polymorphic at the boundary of the selection mosaic ($x = 0$) within mutualistic interactions in an infinite habitat. That is, $\hat{p}(x) = 0$ or 1 at $x = 0$. We will now use this result to estimate the minimum size of a finite region of weak selection $\{0 < x < B\}$ needed to maintain a polymorphic cline. Because $p(x)$ must equal zero or one at $x = 0$, we replace boundary conditions (A3) and (A4) with

$$\frac{d\hat{p}}{dx} = 0 \quad \text{and} \quad \hat{p} \to 0 \text{ or } 1 \quad \text{as } x \to 0 \quad \text{(A10)}$$

and

$$\frac{d\hat{p}}{dx} = 0 \quad \text{and} \quad \hat{p} \to 0 \text{ or } 1 \quad \text{as } x \to -\infty. \quad \text{(A11)}$$

Solving (A1) with these boundary conditions gives solutions with the same maximum slope as equations (10) in the text. Using this slope to approximate the width of the cline leads to equation (11) of the text. Although this derivation is strictly valid only for an infinite habitat, numerical simulations of the discrete time and space model in finite habitats have verified its applicability.

## Appendix 2

Conditions for the stability of a fixed mutualism.

Here we derive conditions for the stability of the equilibria corresponding to the fixed mutualism with $\hat{p}_1(x) = \hat{p}_2(x) = 0$ for all $x$ in an interaction that varies geographically between antagonism and mutualism. Analysis of the alternative fixed mutualism $\hat{p}_1(x) = \hat{p}_2(x) = 1$ is similar. Considering an interaction that is antagonistic ($c_L > 0$, $b_L < 0$) on the interval $\{-A < x < 0\}$ but mutualistic ($c_R$, $b_R > 0$) on the interval $\{0 < x < B\}$ leads to

$$\frac{\partial p_1(x, t)}{\partial t} = \begin{cases} \frac{l_1^2}{2}\frac{\partial^2 p_1}{\partial x^2} + c_L p_1(1 - p_1)(2p_2 - 1) & \{-A < x < 0\} \\ \frac{l_1^2}{2}\frac{\partial^2 p_1}{\partial x^2} + c_R p_1(1 - p_1)(2p_2 - 1) & \{0 < x < B\} \end{cases} \quad \text{(A12)}$$

and

$$\frac{\partial p_2(x, t)}{\partial t} = \begin{cases} \frac{l_2^2}{2}\frac{\partial^2 p_2}{\partial x^2} - b_L p_2(1 - p_2)(2p_1 - 1) & \{-A < x < 0\} \\ \frac{l_2^2}{2}\frac{\partial^2 p_2}{\partial x^2} + b_R p_2(1 - p_1)(2p_2 - 1) & \{0 < x < B\}. \end{cases} \quad \text{(A13)}$$

Rescaling equations (A12) and (A13) with $\xi = x/A$ and linearizing around the equilibrium $\hat{p}_1(x) \equiv \hat{p}_2(x) \equiv 0$ results in

$$\frac{\partial p_1(\xi, t)}{\partial t} = \begin{cases} \frac{l_1^2}{2A^2}\frac{\partial^2 p_1}{\partial \xi^2} + c_L p_1 & \{-1 < \xi < 0\} \\ \frac{l_1^2}{2A^2}\frac{\partial^2 p_1}{\partial \xi^2} + \alpha_1 c_L p_1 & \{0 < \xi < \gamma\} \end{cases} \quad \text{(A14)}$$

and

$$\frac{\partial p_2(\xi, t)}{\partial t} = \begin{cases} \frac{l_2^2}{2A^2}\frac{\partial^2 p_2}{\partial \xi^2} + b_L p_2 & \{-1 < \xi < 0\} \\ \frac{l_2^2}{2A^2}\frac{\partial^2 p_2}{\partial \xi^2} - \alpha_2 b_L p_2 & \{0 < \xi < \gamma\}, \end{cases} \quad \text{(A15)}$$

where $\gamma = B/A$, $\alpha_1 = |c_R/c_L|$ and $\alpha_2 = |b_R/b_L|$. Examination of the linearized system (A14) and (A15) reveals that allele frequency changes in the host and symbiont are independent of one another, indicating that their dynamics can be analyzed separately. Furthermore, because we assume that both $c_L$ and $c_R$ are always positive (the symbiont always benefits from the host) equations (A14), describing allele frequency change in the symbiont, show that the equilibrium $\hat{p}_1(x) = 0$ is always stable. We apply the method of separation of variables to equation (A15), such that $p_2(\xi, t) = F(t)G(\xi)$ on $\{-1 < \xi < 0\}$ and $p_2(\xi, t) = K(t)L(\xi)$ on $\{0 < \xi < \gamma\}$, with $F$, $G$, $K$, and $L$ arbitrary functions of either $t$ or $\xi$. Substituting these expressions into (A15) replaces the partial differential equations with a system of four ordinary differential equations

$$\frac{F'(t)}{F(t)} = \lambda_L, \qquad \{-1 < \xi < 0\} \tag{A16}$$

$$\frac{l_2^2}{2A^2}\frac{G''(\xi)}{G(\xi)} + b_L = \lambda_L, \qquad \{-1 < \xi < 0\} \tag{A17}$$

$$\frac{K'(t)}{K(t)} = \lambda_R, \qquad \{0 < \xi < \gamma\} \tag{A18}$$

and

$$\frac{l_2^2}{2A^2}\frac{L''(\xi)}{L(\xi)} - \alpha_2 b_L = \lambda_R, \qquad \{0 < \xi < \gamma\} \tag{A19}$$

where $\lambda_L$ and $\lambda_R$ are arbitrary constants and primes indicate derivatives. Solving the time-dependent equations (A16) and (A18) subject to the initial, and arbitrarily small, perturbations $\epsilon_L(x)$ and $\epsilon_R(x)$ respectively, leads to the exponential solutions

$$F = \epsilon_L(x)e^{\lambda_L t} \quad \text{and} \tag{A20}$$

$$K = \epsilon_R(x)e^{\lambda_R t}, \tag{A21}$$

indicating that the critical values of $\lambda_L$ and $\lambda_R$ for which the initial perturbations $\varepsilon_L(x)$ and $\varepsilon_R(x)$, will neither shrink nor grow is $\lambda_L = \lambda_R = 0$. At the critical values, equations (A16)–(A19) reduce to

$$\frac{G''(\xi)}{G(\xi)} = -\omega_2 A^2 \qquad \{-1 < \xi < 0\} \tag{A22}$$

and

$$\frac{L''(\xi)}{L(\xi)} = \alpha_2\omega_2 A^2, \qquad \{0 < \xi < \gamma\} \tag{A23}$$

where $\omega_2 = |2b_L/l_2^2|$. For a solution to equations (A22) and (A23) to exist, subject to the boundary conditions

$$G'(\xi) = L'(\xi) = 0 \quad \text{at } \xi = -1, \gamma, \tag{A24}$$

$$G(\xi) = L(\xi) \quad \text{at } \xi = 0, \quad \text{and} \tag{A25}$$

$$G'(\xi) = L'(\xi) \quad \text{at } \xi = 0, \tag{A26}$$

it must be true that

$$\omega_2 A^2 < \theta_0, \tag{A27}$$

where $\theta_0$ is the unique root between zero and $\pi/2$ of

$$\tan(\sqrt{\theta_0}) = \sqrt{\alpha_2}\tanh(\gamma\sqrt{\theta_0\alpha_2}). \tag{A28}$$